Hydrology and Earth System Sciences Discussions

Estimation of Mediterranean crops evapotranspiration by means of remote-sensing based models

M. Minacapilli[1], C. Agnese[1], F. Blanda[1], C. Cammalleri[2], G. Ciraolo[2], G. D'Urso[3], M. Iovino[1], D. Pumo[1], G. Provenzano[1], and G. Rallo[1]

[1]Dipartimento di Ingegneria e Tecnologie Agro-Forestali (ITAF), Università di Palermo, Italy
[2]Dept. of Hydraulic Engineering and Environmental Applications, Università di Palermo, Italy
[3]Dept. Agricultural Engineering and Agronomy, University of Naples "Federico II", Italy

Correspondence to: M. Minacapilli (minacap@idra.unipa.it)

Title Page

Abstract   Introduction

Conclusions   References

Tables   Figures

◄   ►

◄   ►

Back   Close

Full Screen / Esc

Printer-friendly Version

Interactive Discussion

Estimation of Mediterranean crops evapotranspiration

M. Minacapilli et al.

Abstract

Actual evapotranspiration from typical Mediterranean crops has been assessed in a Sicilian study area by using Surface Energy Balance and Agro-Hydrological models. Both modelling approaches require remotely sensed data to estimate evapotranspiration fluxes in a spatially distributed way. The first approach exploits visible (VIS), near-infrared (NIR) and thermal (TIR) observations to solve the surface energy balance equation. To this end two different schemes have been tested: the two-sources TSEB model, where soil and vegetation components of the surface energy balance are treated separately, and the widely used one-source SEBAL model, where soil and vegetation are considered as a sole source. Actual evapotranspiration estimates by means of the two surface energy balance models have been compared with the results of the Agro-Hydrological model SWAP, applied in a spatially distributed way to simulate one-dimensional water flow in the soil-plant-atmosphere continuum. In this latter model, remote sensing data in the VIS and NIR spectral ranges have been used to infer spatially distributed vegetation parameters needed to set up the upper boundary condition of SWAP. In the comparison presented here, actual evapotranspiration values obtained from the application of the soil water balance model SWAP have been considered as the reference.

Considering that the study area is characterized by typical Mediterranean sparse vegetation, i.e. olive, citrus and vineyards, we focused the attention on the main conceptual differences between SEBAL and TSEB. Airborne hyperspectral data acquired during a NERC campaign in 2005 have been used. The results of the investigation evidenced that the remote sensing two-sources approach used in TSEB model describes turbulent and radiative surface fluxes in a more realistic way than the one-source approach.

1 Introduction

The estimation of temporal and spatial distribution of actual evapotranspiration (ET) is an essential step for mapping crop water requirements and for water management purposes, especially in Mediterranean areas where water scarcity and semiarid climate cause often fragility and severe damage in the agro-ecosystems. The determination of ET in water-limited conditions is not an easy task, due to the heterogeneity and complexity of involved hydrological and biophysical processes. During recent years, several procedures and models have been developed to simulate mass and energy exchange in the Soil-Plant-Atmosphere (SPA) system (Feddes et al., 1978; Bastiaanssen et al., 2007). In particular, deterministic models have been proposed for detailed simulation of all the components of the water balance, including crop growth, irrigation and solute transport (Vanclooster et al., 1994; van Dam et al., 1997; Droogers et al., 2000; Ragab, 2002). These models have been developed for site-specific applications but they have seldom been applied to large areas, due to the complexity in the acquisition of input data, often characterised by spatial and temporal variability. To overcome this problem, techniques have been suggested which involve the use of GIS (Liu et al., 2007a, b; Liu, 2009) and Remote Sensing techniques to gather quantitative information on the temporal and spatial distribution of various vegetation parameters, i.e. albedo, crop coefficient, leaf area index (Choudhury et al., 1994; D'Urso et al., 1999; Schultz and Engman, 2000). These studies are based on the fact that crop canopy reflects solar radiation, which can be measured with a radiometer at various wavelength in the visible and near-infrared (VIS/NIR) spectral range. The feasibility of using remotely sensed crop parameters in combination of Agro-Hydrological models has been investigated in several studies (D'Urso, 2001; D'Urso and Minacapilli, 2006; Immerzeel et al., 2008; Crown et al., 2008; Minacapilli et al., 2008) with the aim of enabling the spatially distributed evaluation of water balance components in the SPA system.

A further contribution offered by Remote Sensing techniques has been the development of operational methods for the direct estimation of actual evapotranspiration

Estimation of Mediterranean crops evapotranspiration

M. Minacapilli et al.

based on the Surface Energy Balance (SEB) approach, which exploits thermal infrared (TIR) observations of the Earth's surface acquired from satellite and/or airborne platforms (Norman et al., 1995; Chehbouni et al., 1997; Bastiaanssen et al., 1998a, b; Su, 2002). In the recent years, several SEB schemes have been developed (Schmugge et al., 2002) with varying degree of complexity. In all these schemes the evapotranspiration is derived in terms of latent heat flux, λET ($W\,m^{-2}$), ad it is computed as the residual of the surface energy balance equation:

$$\lambda ET = R_n - G_0 - H \tag{1}$$

where R_n ($W\,m^{-2}$) is the total net radiation, G_0 ($W\,m^{-2}$) is the soil heat flux, and H ($W\,m^{-2}$) is the sensible heat flux.

The largest uncertainty in estimating λET is due to the computation of H. Following the bulk resistance or "one-source" approach for a natural surface, the basic equation for soil-plus-canopy sensible heat flux, H, is given by:

$$H = \frac{\rho c_p (T_{0h} - T_a)}{R_a + R_{ex}} = \frac{\rho c_p (T_{0h} - T_a)}{R_{ah}} \tag{2}$$

where ρ ($kg\,m^{-3}$) is the air density, c_p is the specific heat of air ($J\,kg^{-1}\,K^{-1}$), T_{0h} (K) is the so-called "aerodynamic surface temperature" (Kalma and Jupp, 1990), defined as the air temperature *"which satisfies the bulk resistance formulation for sensible heat transport, H"* (Kustas et al., 2007), T_a (K) is the air temperature at some reference height, R_a ($s\,m^{-1}$) is the aerodynamic resistance (Brutsaert, 1982), R_{ex} ($s\,m^{-1}$) is the excess resistance associated with heat transport and R_{ah} ($s\,m^{-1}$) is the total resistance to heat transport across the temperature difference (T_{0h}–T_a). Since the aerodynamic surface temperature is usually unknown, the common approach used in various single-source schemes is to empirically relate the radiative surface temperature, T_r, to T_{0h} or directly to the term (T_{0h}–T_a).

Differently, the so-called "two-sources" approach (Shuttleworth and Wallace, 1985; Shuttleworth and Gurney, 1990; Norman et al., 1995) considers the partitioning of

fluxes in two components, i.e. soil and vegetation, as viewed from a remote sensor with an incidence angle θ. Hence, the total sensible heat flux is given by the sum of H_s, related to soil, and H_c, related to the vegetation canopy:

$$H = H_s + H_c \tag{3}$$

$$H_c = \rho c_p \left[\frac{T_c - T_a}{R_{ah}} \right] \tag{4}$$

$$H_s = \rho c_p \left[\frac{T_s - T_a}{R_s + R_{ah}} \right] \tag{5}$$

In Eqs. (4) and (5) T_c and T_s (K) are, respectively, the canopy and soil aerodynamic temperatures and R_s (s m^{-1}) is the soil resistance to the heat transfer (Goudriaan, 1977; Norman et al., 1995; Kustas and Norman 1999a, b).

In this paper the SEBAL single-source model (Bastiaanssen et al., 1998a, b) and the TSEB two-sources model (Norman et al., 1995) have been applied to determine the surface energy fluxes in an area located in the South West of Sicily and characterized by typical Mediterranean crops.

Of particular interest to this study is the use of airborne high-resolution (3 m×3 m) remote sensing data in the VIS/NIR and TIR regions providing a detailed observation of spectral reflectance and surface temperature. The remote acquisition has been taken during an intensive field campaign carried out in 2005, where intensive data including soil and hydrological measurements have been collected. This intensive field data set has been used to implement the soil water balance model SWAP (van Dam et al., 1997) in a spatially distributed way. The spatial distribution of canopy parameters has been derived from airborne observations in the visible and near-infrared ranges, and it has been used to define the upper boundary condition of the SWAP model (D'Urso et al., 1999). The output of the spatially distributed SWAP includes actual evapotranspiration calculated from the root water uptake, validated by means of soil water content measurements. As such, these ET values have been considered as the "reference" in the comparison between SEBAL and TSEB energy balance models, in

absence of a sufficiently dense network of flux instrumentations installed in the study area, which would have been impossible to install in an efficient way due to the high level of agricultural fragmentation.

2 Models description

SEBAL, TSEB and SWAP models use different approaches to calculate actual evapotranspiration. Key differences and peculiarities of the models are described in the following subsections.

2.1 SEBAL and TSEB models

A first application of the models in the same study area can be found in Ciraolo et al. (2006) and in Minacapilli et al. (2007). A detailed description of SEBAL and TSEB models can be found in Norman et al. (1995), Bastiaanssen et al. (1998a, b), Kustas and Norman (1999a, b). Here we only describe the main differences of the models.

In both models, the estimation of total net radiation, R_n, can be obtained by computing the net available energy considering the rate lost by surface reflection in the shortwave (0.3/2.5 µm) and emitted in the longwave (6/100 µm):

$$R_n = (1 - \alpha) R_{swd} + \varepsilon_0 \left(\varepsilon' \sigma T_a^4 - \sigma T_0^4 \right) \tag{6}$$

where R_{swd} (W m^{-2}) is the global incoming solar radiation, α (–) is the surface albedo, ε' is the atmospheric emissivity (–), ε_0 is the surface emissivity (–), σ (W m^{-2} K^{-4}) is the Stefan-Boltzmann constant, T_a (K) is the air temperature, and T_0 (K) is the land surface temperature derivable from thermal remote sensing data. Moreover, the TSEB model splits the net radiation R_n between canopy ($R_{n,c}$) and soil ($R_{n,s}$), that is computed as

a function of Leaf Area Index, LAI ($m^2\,m^{-2}$):

$$R_{n,s} = R_n \exp\left(-0.45\mathrm{LAI}/\sqrt{2\cos(\theta_z)}\right) \tag{7}$$

$$R_{n,c} = R_n - R_{n,s} \tag{8}$$

where R_n is obtained using Eq. (6) and θ_z is the solar zenith angle.

The soil heat flux, G_0 ($W\,m^{-2}$) can be evaluated using different empirical approaches. In the SEBAL model, the value of G_0 is expressed as a fraction of R_n according the following relationship:

$$G_0 = R_n \frac{T_0}{\alpha}\left(0.003\alpha + 0.006\alpha^2\right) \times \left(1 - 0.98\mathrm{NDVI}^2\right) \tag{9}$$

where NDVI (–) is a simple radiometric index derived from red and near infrared bands (Liang, 2004).

In TSEB model, the soil heat flux G_0 is expressed as a fraction c_g (≈ 0.35) of the net radiation at the soil surface $R_{n,s}$.

The estimation of sensible heat flux H obtained solving Eq. (2) for SEBAL model or Eqs. (3–5) for TSEB model requires, the computation of the total aerodynamic resistance, R_{ah}, which in both models can be evaluated by the following equation (Brutsaert, 1982):

$$R_{ah} = \frac{\left[\ln\left(\frac{z_u - d_0}{z_{0,M}}\right) - \Psi_M\right] \cdot \left[\ln\left(\frac{z_T - d_0}{z_{0,H}}\right) - \Psi_H\right]}{k^2 \cdot u} \tag{10}$$

where d_0 (m) is the displacement height, $z_{0,M}$ and $z_{0,H}$ are two roughness parameters (m) that can be evaluated as functions of the canopy height (Shuttleworth and Wallace, 1985), u is the wind speed ($m\,s^{-1}$) measured at height z_u (m), k is the von Karman's constant (≈ 0.4), z_T is the height of the air temperature measurement, Ψ_H (–) and Ψ_M (–) are two stability correction functions for momentum and heat transfer, respectively

(Brutsaert, 1982). A detailed description of the above mentioned parameters can be found in Brutsaert (1982).

As mentioned in the previous paragraph, in the SEBAL model, H is computed via single-source scheme assuming a linear relationship between T_r and $\Delta T = (T_{0h} - T_a)$ to be calibrated on the basis of the knowledge of two boundary conditions identified within the image itself ("anchor" pixels). Hence, a dry non evaporating area is identified and a latent heat flux equal to zero is considered ($H = R_n - G_0$); in a second wet area, i.e. a water body or a fully evaporating surface, it is assumed $H = 0$. In these anchor pixels the ΔT values derived by the inversion of Eq. (2) and the T_r values observed from the TIR remote observation are used to calibrate the coefficients a and b of the following linear relationship:

$$\Delta T = a + bT_r \tag{11}$$

Successively, Eq. (11) is applied to all the image pixels in order to compute ΔT from the corresponding T_r, and hence H by using Eq. (2). Details of the procedure above can be found in Bastiaanssen et al. (1998a, b).

Differently, the two-sources TSEB model considers the contributions from the soil and the canopy separately and it uses a few additional parameters to solve for sensible heat H as the sum of the contribution of the soil, H_s, and of the canopy, H_c, according to Eq. (3). In particular, assuming that the observed radiometric temperature, T_r, is a combination of soil and canopy temperatures, the TSEB model add the following relationship (Becker and Li, 1990) to the set of Eqs. (4) and (5):

$$T_r = \left[f_\theta T_C^4 + (1 - f_\theta) T_S^4 \right]^{1/4} \tag{12}$$

where f_θ is the vegetation directional fractional cover (Campbell and Normann, 1998). Besides the adjustment for the angular dependence of thermal observations, TSEB does not require the linearity assumption introduced in SEBAL through Eq. (11).

The set of Eqs. (4), (5) and (12) includes four unknowns variables (H_c, H_s, T_c, and T_s); as a first approximation, assuming that the vegetation is unstressed and transpiring

at the potential rate, the TSEB model uses the Priestly-Taylor equation (Priestly and Taylor, 1972) to estimate the latent heat flux λET_c as:

$$\lambda ET_c = R_{n,c} - H_c = \alpha_p \frac{\Delta}{\Delta + \gamma} R_{n,c} \qquad (13)$$

where α_p (–) is the Priestly–Taylor parameter, which is initially set to 1.26 ("potential" condition) and progressively adjusted, as explained below. In Eq. (13) Δ is the slope of the saturation vapour pressure-temperature curve at T_C (Pa K^{-1}) and γ is the psychrometric constant. Using Eq. (8) to compute $R_{n,c}$, Eq. (13) is solved for H_c and then Eq. (4) is inverted to estimate T_C as:

$$T_c = \left(1 - \alpha \frac{\Delta}{\Delta + \gamma}\right) R_{n,c} \frac{r_c}{\rho c_p} + T_a \qquad (14)$$

The constraint in Eq. (12) can then be inverted to estimate T_s as:

$$T_s = \left(\frac{T_r^4 - f_\theta T_c^4}{1 - f_\theta}\right)^{1/4} \qquad (15)$$

Prediction of T_s allows for calculation of H_s via Eq. (5) using, for R_s, a relationship suggested by the Authors in the original paper of the model (Norman et al., 1995; Kustas and Norman 1999a, b). Consequently the soil evaporation E_s can be computed as:

$$E_s = G_0 - H_s = c_g R_{n,s} - H_s \qquad (16)$$

If the vegetation canopy is undergoing water stress, Eq. (13) will lead to an overestimation of λET_c, which turns in a negative value of E_s in Eq. (16). This problem is addressed by iteratively decreasing α_p in Eq. (13) until a positive E_s is reached (Kustas and Norman, 1999).

For both the models, once the R_n, G_0 and H spatial distributions are obtained, the λET (W m^{-2}) spatial distribution is computed using Eq. (1). Finally, the daily evapotranspiration ET$_d$ (mm d^{-1}) can be obtained by the time integration of λET using the evaporative fraction parameter, Λ (Menenti and Choudhury, 1993):

$$\Lambda = \frac{\lambda\text{ET}}{R_n - G_0} \tag{17}$$

Several studies (Brutsaert and Sugita, 1992; Crago, 1996) demonstrated that, within daytime hours, the $\Lambda(0-1)$ values are almost constant in time. This fact suggests to use the Λ parameter as a temporal integration parameter. Following this hypothesis, the daily evapotranspiration, ET$_d$ (mm d^{-1}), can be derived using the equation:

$$\text{ET}_d = \Lambda \frac{R_{n,24}}{\lambda} \tag{18}$$

where λ (MJ kg^{-1}) is the latent heat of vaporization and $R_{n,24}$ represents the averaged net daily radiation, that can be derived by direct measurement or by using the classical formulation proposed in FAO 56 paper (Allen et al., 1998).

2.2 The agro-hydrological SWAP model

SWAP (Soil-Water-Atmosphere-Plant) is a one-dimensional physically based model for water, heat and solute transport in saturated and unsaturated soil, and includes modules to simulate irrigation practice and crop growth (Kroes and van Dam, 2003). SWAP simulates the vertical soil water flow and solute transport in close interaction with crop growth. Richards' equation (Richards, 1931), including root water extraction, is applied to compute transient soil water flow:

$$C(h)\frac{\partial h}{\partial t} = \frac{\partial}{\partial z}\left[K(h)\left(\frac{\partial h}{\partial z} + 1\right)\right] + S(h) \tag{19}$$

under specified upper and lower boundary conditions. In Eq. (19) z (cm) is the vertical coordinate, assumed positive upwards, t (d) is time, C (cm^{-1}) is the differential moisture

10

Estimation of Mediterranean crops evapotranspiration

M. Minacapilli et al.

capacity, $K(h)$ (cm d^{-1}) is the soil hydraulic conductivity function and S (d^{-1}) is the root uptake term that, in the case of uniform root distribution, is defined by the following equations:

$$S(h) = \alpha_w(h)\frac{T_p}{|z_r|} \tag{20}$$

$$T_p = K_c \times ET_0 \left[1 - \exp(-K_{gr}LAI)\right] \tag{21}$$

in which T_p (cm d^{-1}) is the potential transpiration, z_r (cm) is the rooting depth and α_w (–) is a h-dependant reduction factor which accounts for water deficit and oxygen stress (Feddes et al., 1978), K_c (–) is the crop coefficient, ET_0 (cm d^{-1}) is the reference evapotranspiration and K_{gr} (–) is an extinction coefficient for global solar radiation. The numerical solution of Eqs. (19), (20) and (21) is possible after specifying initial, and upper and lower boundary conditions and the soil hydraulic properties, i.e. the soil water retention curve, $\theta(h)$, and the soil hydraulic conductivity function, $K(h)$ are known; detailed field and/or laboratory investigations are therefore needed.

In this study, the application of SWAP has been carried out in a spatially distributed way, according to the procedure suggested by D'Urso (2001). The study area has therefore been discretized in individual one-dimensional units, with homogenous soil and canopy parameters. Canopy parameters such crop coefficient, K_c, and the leaf area index, LAI, have been determined by using the remote sensing approach proposed by D'Urso et al. (1999, 2001). Thus, for a given set of climatic variables, using the above mentioned approach, the spatial distributions of the potential evapotranspiration has been derived, and this information has been used to define – in each elementary unit – the upper boundary condition of the soil water balance model SWAP, represented by Eq. (21). A detailed description of the entire procedure can be found in D'Urso (2001) and in Minacapilli et al. (2008).

3 Case study and data collection

The study area covers an extension of approximately 20 ha, located in the south-western coast of Sicily (Fig. 1). Orchard crops (mainly olives, grapes and citrus) represent the dominant vegetation; soil can be classified as silty clay loam (USDA classi-fication). During 2005, daily meteorological data (incoming short-wave solar radiation, air-temperature and humidity, wind speed and rainfall) have been acquired with stan-dard meteorological instrumentations. A soil survey has been carried out to identify the main soil hydraulic parameters, needed as input in SWAP. In particular temporal vari-ability of soil moisture contents in the different plots (Fig. 1) and at different depths were measured using TDR techniques and Diviner 2000 Sentek capacitive sensors. These values have been used for validating SWAP in selected locations. Canopy parameters and radiometric surface temperatures have been acquired during a airborne campaign supported by NERC (National Environment Research Council, UK).

3.1 Aircraft remote sensing pre-processing

The NERC airborne campaign has taken place on 16 May 2005 at about noon (local time). The flight altitude of 1400 m and the optical characteristics of the ATM sensor (Airborne Thematic Mapper) has produced images with a nominal spatial resolution (pixel size) of 3×3 m. ATM has 8 spectral bands in the visible and near-infrared ranges (VIS/NIR) 2 in the short-wave infrared (SWIR) and 1 in the thermal infrared region (TIR). At the same time of the acquisition flight, a field survey was carried out by mea-suring spectral and vegetation parameters in correspondence of predefined homoge-neous targets. Spectral measurements on water, bare soil and grass surfaces have been acquired by using an ASDI FieldSpect HH spectroradiometer; these measure-ments have been used for the radiometric and atmospheric corrections of the VIS-NIR images of ATM by using the empirical line method (Slater et al., 1996). The result-ing surface reflectance values have been successively used to calculate the surface albedo and the vegetation indexes. At-surface temperature measurements have been

made in selected locations simultaneously to the flight, in order to perform an empirical calibration of the thermal images acquired by the ATM sensor. Figure 2a and b shows the accuracy obtained from the abovementioned corrections in both VIS/NIR and TIR bands. The geometric correction of the entire data set has been performed using the NERC Azgcorr software, that performs geocorrection of images using aircraft navigation data and Digital Elevation Model (DEM) of the acquired zone.

3.2 SWAP model parameterization

The minimum data-set required for the application of the SWAP model includes four main information types: i) soil hydraulic parameters; ii) lower boundary condition, defined by the groundwater table or the water flux to or from an existent aquifer; iii) parameters related to the upper boundary, i.e. rainfall and/or potential evapotranspiration; iv) soil moisture content or soil water pressure head profile for the initial condition.

Maps of soil hydraulic properties have been realised by means of a soil survey with an intensive undisturbed sampling. Laboratory investigations on the undisturbed soil cores have been carried to determine the soil water hydraulic and retention curves required in input for SWAP. The saturated hydraulic conductivity, K_s (cm d^{-1}) has been determined by means of the constant head technique (Reynolds et al., 2002); soil water content θ has been determined in correspondence of a set of pressure head values, h, ranging from -5 to $-15\,300$ cm by means of a hanging water column apparatus (Burke et al., 1986) and a pressure plate apparatus (Dane and Hopmans, 2002). The water retention function of van Genuchten (1980) has been fitted to the measured θ-h values by using the RETC (RETention Curve) code (van Genuchten et al., 1991). The unsaturated hydraulic conductivity function has been derived by using the Mualem-van Genuchten model (van Genuchten, 1980). Due to the limited spatial variability of soil properties, it has been possible to consider an unique soil profile for the simulations of soil water balance in the study area, which characteristics are summarised in Table 1.

The intensive field measurements collected during 2005 showed that the soil water content was always near to saturated value from 1.2 m to lower depths. Therefore, the

simulations were carried out considering a zero flux at the bottom of the soil profile.

The upper boundary condition, in terms of potential evapotranspiration ET_p (mm d^{-1}) was obtained by multiplying the reference evapotranspiration (ET_0) with the crop coefficients (K_c). The ET_0 was determined by using the Penman-Monteith equation (Allen et al., 1998), while the spatial distribution of the crop coefficients was obtained using the remote sensing approach proposed by D'Urso (2001). As mentioned in Sect. 2.2, the procedure requires the knowledge of canopy parameters such as the surface albedo, α, the leaf area index, LAI, the crop height h_c, and the standard set of meteorological data (wind speed at reference height, shortwave incoming solar radiation, air temperature and humidity). For the study area, the crop parameters have been derived using spectral reflectance values acquired from the ATM VIS/NIR bands. In particular, the surface albedo have been computed as weighted average over VIS and NIR spectrum assuming as weighting parameter the solar irradiance for each bandwith (Liang, 2004). The LAI spatial distribution has been detected using the following semi-empirical relationship (Clevers, 1989):

$$\mathrm{LAI} = -\frac{1}{\alpha^*} \ln \left(1 - \frac{\mathrm{WDVI}}{\mathrm{WDVI}_\infty} \right) \tag{22}$$

in which WDVI is a vegetation index derived from ATM red and near-infrared bands (Clevers, 1989), WDVI_∞ is the asymptotic value of WDVI for LAI$\to\infty$, and α^* is an extinction coefficient, denoting the increase of LAI for a unit increase of WDVI, that has to be estimated from simultaneous measurements of LAI and WDVI. In our case, the calibration of Eq. (22) was preliminarily carried out by in-situ LAI measurements collected with the portable instrument LAI2000 (Li-Cor, Lincoln, NE). A complete description of the leaf area index estimation conducted for the study area is given in Minacapilli et al. (2005, 2008). Otherwise, as suggested by other authors (Anderson et al., 2004) the crop heigh, h_c, has been calculated using a polynomial relationship derived from field data of LAI and h_c. Once derived α, LAI and h_c crop parameters, the pixel based spatial distribution of crop coefficients K_c has been derived for the date of the NERC airborne overflight (16 May 2005, J=135) with the resolution of $3\,\mathrm{m} \times 3\,\mathrm{m}$

Title Page

Abstract | Introduction

Conclusions | References

Tables | Figures

◄ | ►

◄ | ►

Back | Close

Full Screen / Esc

Printer-friendly Version

Interactive Discussion

(Fig. 3a); afterwards the values were spatially aggregated using a regular vector grid having a mesh size of 15 m×15 m (Fig. 3b) and corresponding to the set of single units that will be used for the spatially distributed application of SWAP model.

Considering that, with the exception of the grape, all the other crops in the study area are evergreen, the only ATM airborne surveys, acquired on 16.05.2005 has been sufficient to derive crop coefficients values as input in the SWAP simulation period (15.04.2005–15.05.2005). At the starting date, a lumped value of the crop coefficient for grape was derived from specific literature (Allen et al., 1998) by assuming a linear variation during the period of simulation.

Others crop parameters required by SWAP, i.e. k_{gr}, z_r and the critical pressure head values defining the reduction factor α_w in Eq. (20), were taken from specific literature (Taylor and Ashcroft, 1972; Doorenbos and Kassam, 1979; Wesseling et al., 1991) with some minor adaptations based on local observations. Crop parameters for the case study used for the simulations are summarized in Table 2.

4 Results and discussion

The following results focus on the crop evapotranspiration estimated using both energy (SEBAL and TSEB) and soil-water (SWAP) balance modelling approaches. In paragraph 4.1, a preliminary validation of SWAP model at field scale is discussed; afterwards the application of SWAP model has been replicated in a distributed way using the approach described in paragraph 3.2. Finally, in paragraph 4.2 evaluation of the spatially patterns of surface energy fluxes and evapotraspiration values predicted by SEBAL and TSEB models is showed, as well as the final comparison of spatially distributed crop evapotranspiration estimated with the three different approaches.

4.1 Validation of SWAP at field scale and its spatially distributed application

The validation of SWAP has been carried out in correspondence of three different locations, inside the experimental farm (Fig. 1), where measurements of soil water content have been continuously acquired during the simulation period. Mean K_c values for the
5   different crop types at these locations – and extracted from the map in Fig. 3a – are summarized in Table 2. As evidenced in the plots of Fig. 4, a good agreement has been found between measured and simulated soil water content; a more complete description of the validation procedures of SWAP model at field scale can be found in Blanda (2007).
10   From the application of the SWAP model to the study area, we have simulated the actual evapotranspiration for each elementary unit on a daily basis; an example of the resulting map for the simulation day corresponding to the NERC flight is shown in Fig. 5. A summary of the values obtained for each crop type is given in Table 3. From Fig. 5, we may notice a significant spatial variability in evapotranspiration in the olive orchard,
15   as highlighted by the higher coefficient of variation (34.8%). This behaviour is driven largely by variations of the fraction of ground covered by canopy (fraction cover) inside each 15 m×15 m simulated unit. Otherwise for the citrus grove the greater uniformity of the fraction cover involves a lower spatial variability in evapotranspiration patterns. On the same date the vineyards was less developed so that less evapotranspiration rates
20   was recognized.

4.2 Estimating ET by SEB models and final comparison

The two surface energy balance models, i.e. SEBAL and TSEB, have been applied by using VIS/NIR and TIR data acquired during the NERC campaign on 16 May 2005 as described in Sect. 3.1. The output of these models has been compared in terms of
25   spatial patterns of actual ET, as well as in terms of statistical correlation on a pixel-by-pixel basis. The resulting maps of ET, as displayed in Fig. 6a and b, have been produced with a spatial resolution of 3 m; thanks to this high spatial resolution of TIR

data, it is possible to observe in great detail the spatial patterns of ET, which may improve the interpretation of the model results. The plot in Fig. 7 is a pixel-wise scatterplot of the daily ET values obtained with the two models. This plot evidences that SEBAL produces an underestimation of ET compared to TSEB of about $1\,\mathrm{mm\,d^{-1}}$. This under-
estimation can be explained by giving a closer look to the values of the different terms of the energy balance, as shown by Fig. 8, where maps and scatterplots of sensible heat flux H and soil heat flux G are represented. From this figure, we may notice that SEBAL gives a systematic strong overestimation of H, which is not compensated by the opposite behaviour of G. This effect, which has been already observed in other
similar studies (Savige et al., 2005; Ciraolo et al., 2006; Minacapilli et al., 2007), has been related to an underestimation of the total resistance to the heat transport over sparsely vegetated surface, since SEBAL does not take into account the soil–canopy interactions. Diversely, TSEB model based on the partitioning between soil and canopy is able to provide a more physically-based picture of the surface resistances involved.
As a result, being the available energy (R_n–G) quite similar between the two models, the overestimation of sensible heat flux in SEBAL is mainly responsible for the disagreement in λET shown in Fig. 7.

In the first phase, assuming the actual evapotranspiration values simulated by SWAP as reference, the ET values obtained using SEBAL and TSEB models have been spatially aggregated by using the same $15\,\mathrm{m}\times15\,\mathrm{m}$ grid adopted in the SWAP simulation.

A further comparison has then been carried out by considering the spatial distribution of the different values of ET, as shown by Fig. 9a and b. Again, we notice that the different scale does not compensate for the difference in ET between TSEB and SEBAL, already observed at $3\,\mathrm{m}\times3\,\mathrm{m}$ pixel resolution.

Finally, an assessment of models performances were evaluated computing the difference MD (mm/d) between the actual ET obtained by means of SEBAL/TSEB and SWAP.

Maps presenting the spatial distribution of MD values are shown in Fig. 9c and d: for both models MD values range from −2.5 to 2.5 mm/d with a smaller mean value using

Estimation of Mediterranean crops evapotranspiration

M. Minacapilli et al.

TSEB (−0.14 mm/d) compared to SEBAL (−0.55 mm/d). The MD spatial distributions allow to identify where the largest discrepancies occur: for citrus and vineyard similar differences for both models, but with a lesser extent for the TSEB, can be observed. Olive fields are however characterized by larger discrepancies in the spatial patterns.

⁵ The analysis of frequency distribution of MD values, shown in Fig. 10a–c, evidences that these discrepancies are related to canopy fragmentation. This phenomena can be explained using different classes of LAI, i.e. over sparsely vegetated surfaces (0.5<LAI<2.5) the largest discrepancies between one- and two source approaches are particularly evident since SEBAL does not split energy fluxes into soil and vegetation ¹⁰ components.

Figure 11 shows the comparison between crop average evapotranspiration ET obtained with SWAP, SEBAL and TSEB models. Also from this type of comparison a better agreement can be recognized between SWAP and TSEB, whereas a general underestimation of ET values is obtained using SEBAL. For the vineyard both TSEB and ¹⁵ SEBAL ET values are equally underestimated compared with the values evaluated with SWAP. This behaviour might be due to the initial development stage of vineyard on 16/05 with low LAI and a strong row architecture of the plants, causing high values of radiometric temperatures influenced by the bare soil rather than the canopy.

5 Conclusions

²⁰ The main aim of this study was the assessment of actual crop evapotranspiration rates, ET, derived using both surface energy balance and agro-hydrological modelling approaches. Since we focused on the evaluation of ET in a spatially distributed manner, two algorithms (SEBAL and TSEB), specifically developed as Remote Sensing based surface energy balance models, were tested. Regarding the agro-hydrological mod-
²⁵ elling approach, a procedure combining the agro-hydrological SWAP model with high resolution remote sensing data, allowing to simulate in a spatially distributed way all the components of water balance in Soil Plant Atmosphere system, was applied. The

choice to use this type of comparison has been driven by the awareness of difficulties in performing flux field measurements to directly validate surface energy balance models, i.e. eddy covariance or scintillometer techniques, especially in agricultural areas with high level of crop fragmentation. Agro-hydrological approaches based on mass water balance, such as the SWAP model, instead provide the opportunity to validate and/or calibrate the estimates of the soil water balance system, using spatial soil water measurements.

In the present paper the crop evapotranspiration values estimated with SEBAL and TSEB models are compared to the values obtained with the Agro-Hydrological SWAP model. Using the procedure suggested by D'Urso (2001), the SWAP model has been applied in a spatially distributed way, and the actual evapotranspiration outputs have been used as references value for the comparison between SEBAL and TSEB.

Considering that the study area is characterized by typical Mediterranean sparse vegetation, i.e. olive, citrus and vineyards, we focused at the main conceptual differences between SEBAL "single-source" and TSEB "two-sources". The results of the investigation indicated that the remote sensing two-source approach used in TSEB model represents turbulent and radiative surface fluxes in a more realistic way than the one-source approach. Using spatially distributed evapotranspiration estimates obtained by an accurate application of SWAP the largest discrepancies between TSEB and SEBAL occurred over sparsely vegetated areas, where TSEB provides a more accurate estimate of spatial variability of aerodynamic surface resistance of the coupled soil/canopy system.

Back | Close

Full Screen / Esc

Printer-friendly Version

Interactive Discussion

References

Allen, R. G., Pereira, L. S., Raes, D., and Smith, M.: Crop evapotranspiration. Guidelines for computing crop water requirements. FAO Irrigation and Drainage Paper (56), Rome, Italy, 1998.

5 Anderson, M. C., Neale, C. M. U., Li, F., Norman, J. M., Kustas, W. P., Jayanthi, H., and Chavez, J.: Upscaling ground observations of vegetation water content, canopy height, and leaf area index during SMEX02 using aircraft and Landsat imagery, Remote Sens. Environ., 92, 447–464, 2004.

Bastiaanssen, W. G. M., Menenti, M., Feddes, R. A., and Holtslag, A. A. M.: The Surface
10 Energy Balance Algorithm for Land (SEBAL): Part 1 formulation, J. Hydrol., 212/213, 198–212, 1998a.

Bastiaanssen, W. G. M., Pelgrum, H., Wang, J., Ma, Y., Moreno, J., Roerink, G. J., and van der Wal, T.: The Surface Energy Balance Algorithm for Land (SEBAL): Part 2 validation, J. Hydrol., 212/213, 213–229, 1998b.

15 Bastiaanssen, W. G. M., Allen, R. G., Droogers, P., D'Urso, G., and Steduto, P.: Twenty-five years modeling irrigated and drained soils: State of the art, Agr. Water Manage., 92, 111–125, 2007.

Becker, F. and Li, Z. L.: Temperature-independent spectral indices in thermal infrared bands, Remote Sens. Environ., 32, 17–33, 1990.

20 Blanda, F.: Indagini sperimentali e modellistica dei processi agroidrologici di colture tipiche dell'ambiente mediterraneo (Experimental researches and agrohydrological modeling of typical Mediterranean crops, PhD thesis dissertation), Università di Palermo, Dottorato in Idronomia Ambientale, 124 pp., 2005 (in Italian with English abstract).

Brutsaert, W. and Sugita, M.: Regional surface fluxes from satellite-derived surface tempera-
25 tures (AVHRR) and radiosonde profiles, Bound. Layer Met., 58, 355–366, 1992.

Brutsaert, W.: Evaporation into the Atmosphere. Theory, History and Applications. D. Reidel Publ. Co., Dordrecht, The Netherlands, 1982.

Burke, W., Gabriels, D., and Bouma, J.: Soil structure assessment. Balkema, Rotterdam, The Netherlands, 1986.

30 Campbell, G. S. and Norman, J. M.: An introduction to environmental biophysics. Springer, New York, 286 pp., 1998.

Chehbouni, A., Nichols, W. D., Njoku, E. G., Qi, J., Kerr, Y., and Cabot, F.: A three component

---

Estimation of Mediterranean crops evapotranspiration

M. Minacapilli et al.

Printer-friendly Version

Interactive Discussion

model to estimate sensible heat flux over sparse shrubs in Nevada, Remote Sens. Rev., 15, 99–112, 1997.

Choudhury, B. J., Ahmed, N. U., Idso, S. B., Reginato, R. J., and Daughtry, C. S. T.: Relations between evaporation coefficients and vegetation indices studied by model simulations, Remote Sens. Environ., 50, 1–17, 1994.

Ciraolo, G., D'Urso, G., and Minacapilli, M.: Actual evapotranspiration estimation by means of airborne and satellite remote sensing data. In: Proc. Remote Sensing for Agriculture, Ecosystems and hydrology VIII, edited by: Owe, M., D'Urso, G., and Neale, C., SPIE Europe, Stoccolma, Italy, 2006.

Clevers, J. G. P. W.: The application of a weighted infrared-red vegetation index for estimating leaf area index by correcting for soil moisture, Remote Sens. Environ., 29, 25–37, 1989.

Crago, R. D.: Conservation and variability of the evaporative fraction during the daytime, J. Hydrol., 180, 173–194, 1996.

Crown, W. T., Kustas, W. P., and Prueger, J. H.: Monitoring root-zone soil moisture through the assimilation of a thermal remote sensing-based soil moisture proxy into a water balance model, Remote Sens. Environ., 112, 1268–1281, 2008.

D'Urso, G., Menenti, M., and Santini, A.: Regional application of one-dimensional water flow models for irrigation management, Agr. Water Manage., 40, 291–302, 1999.

D'Urso, G. and Minacapilli, M.: A semi-empirical approach for surface soil water contentestimation from radar data without a-priori information on surface roughness, J. Hydrol., 321, 297–310, 2006.

D'Urso, G.: Simulation and management of on-demand irrigation systems: a combined agro-hydrological and remote sensing approach, Monography, Wageningen University, ISBN 90-5808-399-3, 174 pp., 2001.

Dane, J. H. and Hopmans, J. W.: Water retention and storage: laboratory, in: Methods of Soil Analysis. Part 4. Physical Methods, edited by: Dane, J. H. and Topp, G. C., Soil Sci. Soc. Am. Book Series No.5. Madison, WI, pp. 688–692, 2002.

Doorenbos, J. and Kassam, A. H.: Yield response to water. FAO Irrigation and Drainage Paper 33, Food and Agricultural Organization of the United Nations, Rome, 1979.

Droogers, P., Bastiaanssen, W. G. M., Beyazgul, M., Kayam, Y., Kite, G. W., and Murray-Rust, H.: Distributed agro-hydrological modeling of an irrigation system in western Turkey, Agr. Water Manage., 43, 183–202, 2000.

Feddes, R. A., Kowalik, P. J., and Zaradny, H.: Simulation of field water use and crop yield,

Estimation of Mediterranean crops evapotranspiration

M. Minacapilli et al.

Monographs, Pudoc (Centre for Agricultural Publishing and Documentation), Wageningen, 189 pp., 1978.

Goudriaan, J.: Crop micrometeorology: a simulation study, Center for Agric. Publ. and Doc., Wageningen, The Netherlands, 1977.

5 Immerzeel, W. W., Gaur, A., and Zwart, S. J.: Integrating remote sensing and a process-based hydrological model to evaluate water use and productivity in a south Indian catchment, Agr. Water Manage., 95, 11–24, 2008.

Kalma, J. D. and Jupp, D. L. B.: Estimating evaporation from pasture using infrared thermometry: evaluation of a one-layer resistance model, Agr. Forest Meteorol., 51, 223–246, 1990.

10 Kroes, J. G., Wesseling, J. G., and van Dam, J. C.: Integrated modelling of the soil-water atmosphere-plant system using the model SWAP 2.0, an overview of theory and an application, Hydrol. Process., 14, 1993–2002, 2000.

Kustas, W. P. and Norman, J. M.: A two-source energy balance approach using directional radiometric temperature observations for sparse canopy covered surface, Agron. J., 92, 847–854, 1999a.

15 Kustas, W. P. and Norman, J. M.: Evaluation of soil and vegetation heat flux predictions using a simple two-source model with radiometric temperature for partial canopy cover, Agr. Forest Meteorol., 94, 13–29, 1999b.

Kustas, W. P., Anderson, M. C., Norman, J. M., and Li, F.: Utility of radiometric-aerodynammic temperature relations for heat flux estimation, Bound.-Lay. Meteorol., 122, 167–187, 2007.

20 Liang, S.: Qantitative Remote Sensing of Land Surface, J. Wiley & Sons, Inc., Publication, 528 pp., 2004.

Liu, J., Williams, J. R., Zehnder, A. J. B., and Yang, H.: GEPIC – modelling wheat yield and crop water productivity with high resolution on a global scale, Agr. Syst., 94(2), 478–493, 2007a.

25 Liu, J., Wiberg, D., Zehnder, A. J. B., and Yang, H.: Modelling the role of irrigation in winter wheat yield and crop water productivity in China, Irrigation Sci., 26(1), 21–33, 2007b.

Liu, J.: A GIS-based tool for modelling large-scale crop-water relations, Environ. Modell. Softw., 24(3), 411–422, 2009.

Menenti, M. and Choudhury, B. J.: Parameterization of land surface evaporation by means 30 of location dependent potential evaporation and surface temperature range, in: Exchange Processes at the Land Surface for a Range of Space and Time Scales, edited by: Bolle, H. J., Feddes, R. A., and Kalma, J. D., pp. 561–568, IAHS Publ. 212, IAHS Press, Wallingford, UK, 1993.

Estimation of Mediterranean crops evapotranspiration

M. Minacapilli et al.

Minacapilli, M., Ciraolo, G., and D'Urso, G.: Evaluating actual evapotranspiration by means of multi-platform remote sensing data: a case study in Sicily, Proceedings of Symposium HS3007 at IUGG2007, Perugia, July 2007, IAHS Publ. 316, 2007.

Minacapilli, M., D'Urso, G., and Qiang, L.: Applicazione e confronto dei modelli SAIL e CLAIR per la stima dell'indice di area fogliare da dati iperspettrali MIVIS (A comparison between SAIL and CLAIR models for LAI estimation from hyperspectral MIVIS data), Riv. Ital. Telerilevamento, 33, 15–25, 2005 (in Italian with English abstract).

Minacapilli, M., Iovino, M., and D'Urso, G.: A distributed agro-hydrological model for irrigation water demand assessment, Agr. Water Manage., 95, 123–132, 2008.

Norman, J. M., Kustas, W. P., and Humes, K. S.: A two-source approach for estimating soil and vegetation energy fluxes in observations of directional radiometric surface temperature, Agr. Forest Meteorol., 77, 263–293, 1995.

Priestley, C. H. B. and Taylor, R. J.: On the assessment of surface heat flux and evaporation using large-scale parameters, Mon. Weather Rev., 100, 81–92, 1972.

Ragab, R.: A holistic generic integrated approach for irrigation, crop and field management: the SALTMED model, Environ. Modell. Softw., 17, 345–361, 2002.

Reynolds, W. D., Elrick, D. E., Young, E. G., Booltink, H. W. G., and Bouma, J.: Saturated and field-saturated water flow parameters: water transmission parameters: Laboratory methods. In: Methods of Soil Analysis. Part 4. Physical Methods, edited by: Dane, J. H. and Topp, G. C., Soil Sci. Soc. Am. Book Series No. 5. Madison, WI, pp. 802–817, 2002.

Richards, L. A.: Capillary conduction of liquids through porous mediums, Physics, 1, 318–333, 1931.

Savige, C., Western, A., Walker, J. P., Kalma, J. D., French, A., and Abuzar, M.: Obtaining surface energy fluxes from remotely sensed data, in: Proc. Modelling and Simulation, edited by: Zerger, A. and Argent, R. M., pp. 2946–2952, MODSIM 2005 Society of Australia and New Zealand, 2005.

Schultz, G. A. and Engman, E. T. (Eds.): Remote Sensing in Hydrology and Water Management, Springer-Verlag Inc., New York, USA, 473 pp., 2000.

Schumugge, T. J., Kustas, W. P., Ritchie, J. C., Jackson, T. J., and Rango, A.: Remote sensing in hydrology, Adv. Water Resour., 25, 1367–1385, 2002.

Shuttleworth, W. J. and Gurney, R. J.: The theoretical relationship between foliage temperature and canopy resistance in sparse crop, Q. J. Roy. Meteorol. Soc., 116, 497–519, 1990.

Shuttleworth, W. J. and Wallace, J. S.: Evaporation from sparse crops – an energy combination

theory, Q. J. Roy. Meteorol. Soc., 111, 839–855, 1985.

Slater, P., Biggar, S., Thome, K., Gellman, D., and Spyak, P.: Vicarious radiometric calibrations of EOS sensors, J. Atmos. Ocean Tech., 13, 349–359, 1996.

Su, Z.: The Surface Energy Balance System (SEBS) for estimation of turbulent heat fluxes, Hydrol. Earth Syst. Sci., 6, 85–100, 2002, http://www.hydrol-earth-syst-sci.net/6/85/2002/.

Taylor, S. A. and Ashcroft, G. M.: Physical Edaphology. The Physics of irrigated and non-irrigated soils, Freeman, San Francisco, CA, 563 pp., 1972.

van Dam, J. C., Huygen, J., Wesseling, J. G., Feddes, R. A., Kabat, P., van Walsum, P. E. V., Groenendijk, P., and van Diepen, C. A.: Theory of SWAP version 2.0. Simulation of water flow, solute transport and plant growth in the Soil-Water-Atmosphere-Plant environment, Technical Document 45, Wageningen Agricultural University and DLO Winand Staring Centre, The Netherlands, 1997.

van Genuchten, M. T., Leij, F. J., and Yates, S. R.: The RETC code for quantifying the hydraulic functions of unsaturated soils. Report No. EPA/600/2-91/065, US Environmental Protection Agency, Office of Research and Development, Washington, D.C., 1991.

van Genuchten, M. T.: A closed form equation for predicting the hydraulic conductivity of unsaturated soils, Soil Sci. Soc. Am. J., 44, 892–898, 1980.

Vanclooster, M., Viane, P., Diels, J., and Christiens, K.: Wave. A mathematical model for simulating water and agrochemicals in the soil and vadose environment. Reference and user's manual (release 2.0), Institute for Land and Water Management, Katholieke Universiteit Leuven, Leuven, Belgium, 1994.

Warrick, A. W. and Nielsen, D. R.: Spatial variability of soil physical properties in the field, in: Application of Soil Physics, edited by: Hillel, D., Academic Press, NY, pp. 319–344, 1980.

Wesseling, J. G., Elbers, J. A., Kabat, P., and van den Broek, B. J.: SWATRE: instructions for input. Internal note, Winand Staring Centre (alterra), Wageningen, The Netherlands, International Waterlogging and Salinity Research Institute, Lahore, Pakistan, 29 pp., 1991.

Wosten, J. H. M., Bannik, M. H., De Gruijter, J. J., and Bouma, J.: A procedure to identify different groups of hydraulic-conductivity and moisture-retention curves for soil horizons, J. Hydrol., 86, 133–145, 1986.

Estimation of Mediterranean crops evapotranspiration

M. Minacapilli et al.

Title Page	
Abstract	Introduction
Conclusions	References
Tables	Figures
◄◄	►►
◄	►
Back	Close
Full Screen / Esc	
Printer-friendly Version	
Interactive Discussion	

**Estimation of Mediterranean crops evapotranspiration**

M. Minacapilli et al.

Table 1. Soil characteristics and hydraulic parameters according to van Genuchten (1980).

Layers depth (cm)	K_s (cm d^{-1})	θ_s (m^3 m^{-3})	θ_r (m^3 m^{-3})	n (–)	α_{mg} (cm^{-1})
0–20	10	0.400	0.030	1.838	0.0104
20–40	3	0.444	0.139	2.128	0.0118
40–60	30	0.400	0.103	1.548	0.0159
60–180	0.24	0.410	0.119	1.487	0.046

Table 2. Main crop parameters used for the simulations in the study area (standard deviation values are given in parentheses).

Parameters	Vineyard	Olive	Citrus
Crop factors K_c			
K_c at simulation starting date (15 Apr 2005)	0.25[a]	0.62 (0.08)	0.75 (0.07)
K_c at simulation ending date (16 May 2005)	0.35 (0.05)	0.62 (0.08)	0.75 (0.07)
Critical pressure heads (cm)			
h_2 (h below which optimum water uptake starts in the root zone)	−25	−25	−25
h_{3h} (h below which optimum water uptake reduction starts in the root zone in case of high atmospheric demand)	−750	−1500	−200
h_{3l} (h below which optimum water uptake reduction starts in the root zone in case of low atmospheric demand)	−1500	−1500	−1000
h_4 (wilting point, no water uptake at lower pressure heads)	−10 000	−16 000	−10 000
Treshold level of high atmospheric demand (mm d^{-1})	5	5	5
Treshold level of low atmospheric demand (mm d^{-1})	2	2	2
k_{gr} (extinction coefficient) (−)	0.45	0.50	0.45
z_r (soil depth where root density is maximum) (cm)	60–70	40–60	40–60

[a] from Allen et al. (1998)

⏮ | ⏭

◀ | ▶

Back | Close

Full Screen / Esc

Printer-friendly Version

Interactive Discussion

Table 3. Crop averaged evapotranspiration components (mm/d) in the day when the airborne overpassed (16 May 2005) obtained using SWAP model; the coefficients of variation (%) are given in parentheses.

Output SWAP		16 May 2005 (J=135)					
		Olive		Vineyard		Citrus	
Actual evaporation	(mm/d)	0.32	(6.2)	0.32	(0.10)	0.32	(3.4)
Actual transpiration	(mm/d)	0.42	(60.5)	0.29	(44.7)	2.59	(30.1)
Actual evapotranspiration	(mm/d)	0.74	(34.8)	0.61	(21.2)	2.91	(26.8)
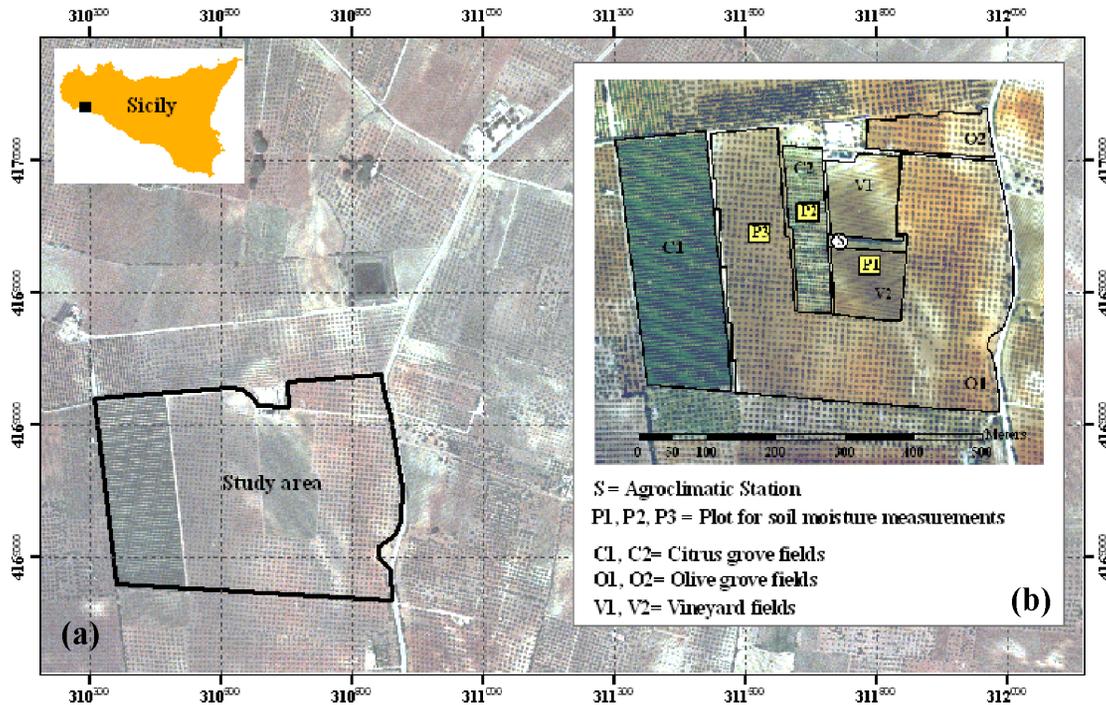
Fig. 1. Geographic location of the study area **(a)** with description of landuse and plots where the soil moisture measurements were acquired **(b)**.
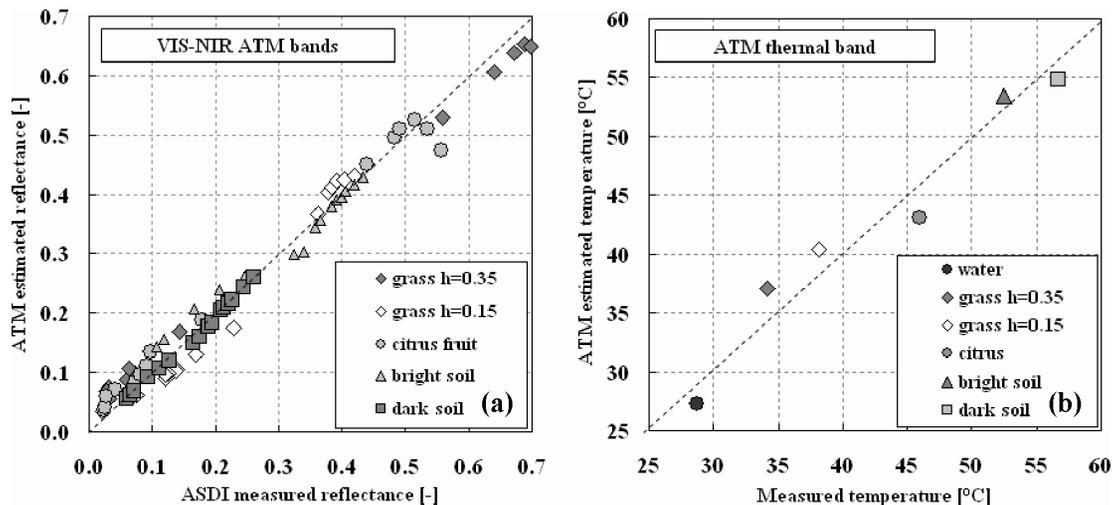
Fig. 2. Validation of correction procedures used to calibrate **(a)** VIS-NIR and **(b)** TIR ATM bands.
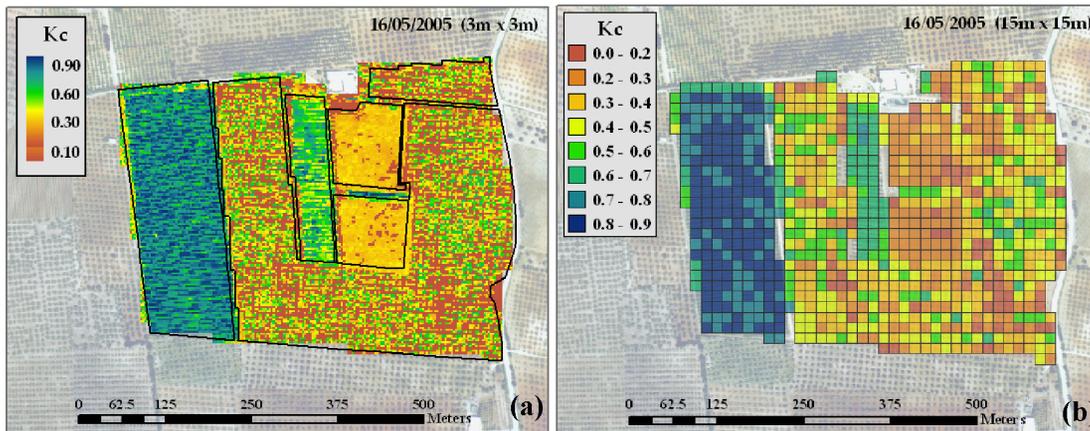
Fig. 3. Spatial distributions of crop factor, K_c, derived from the ATM image of 16.05.2005: **(a)** values at the spatial resolution of airborne image (3 m×3 m) and **(b)** aggregated using the grid reference of 15 m×15 m resolution used for the application of SWAP model in a spatially distributed way.
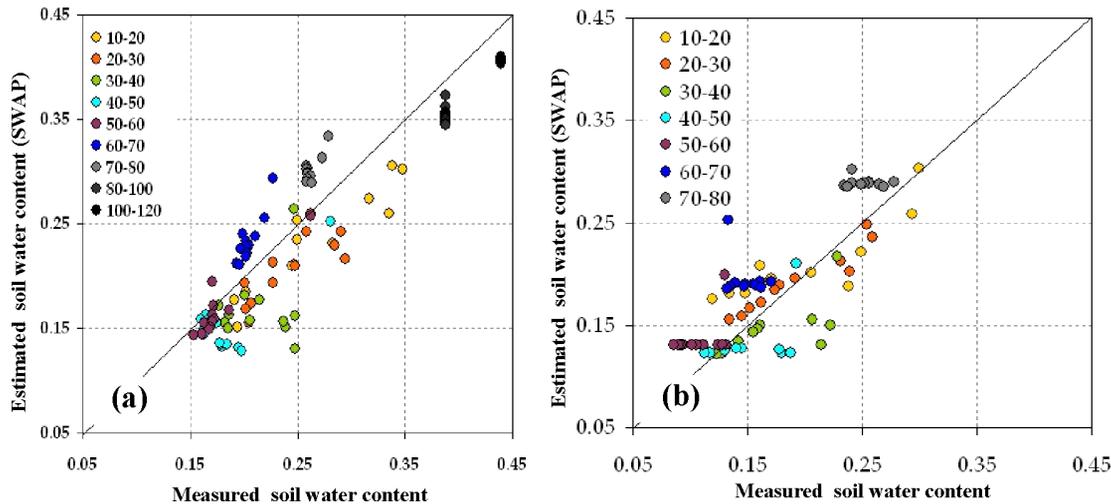
Fig. 4. Soil water balance validation at field scale: Comparison of simulated versus measured multitemporal soil water content at different soil depths (cm); **(a)** Olive crop; **(b)** Vineyards crop.
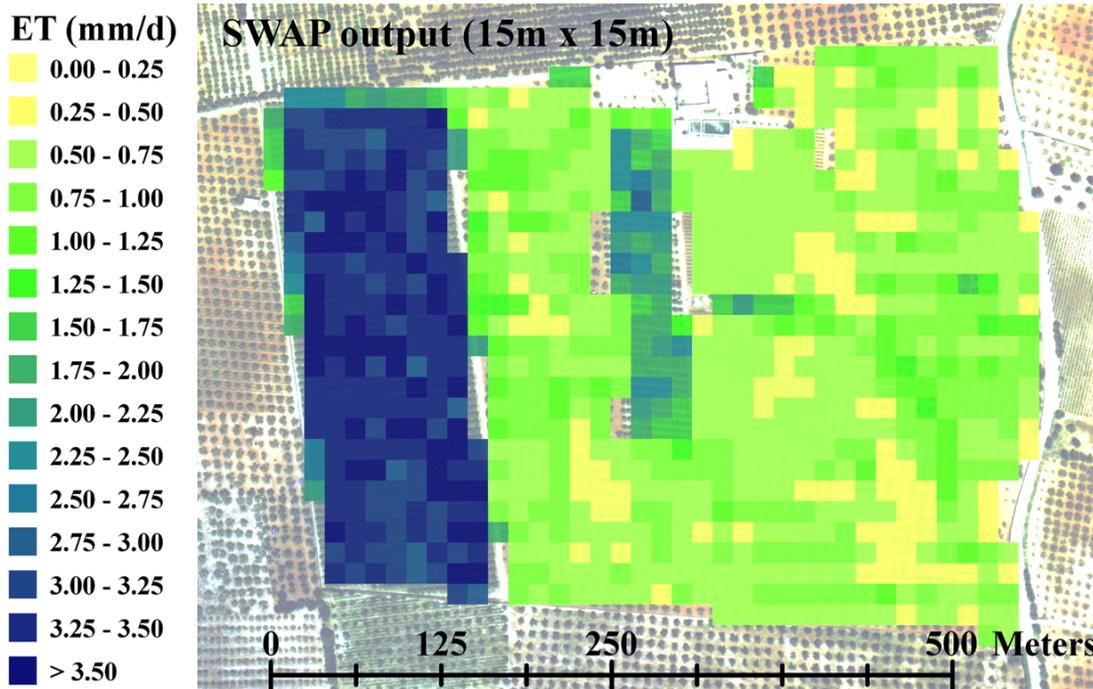
Fig. 5. Daily actual evapotranspiration map obtained from SWAP model on 16 May 2005.
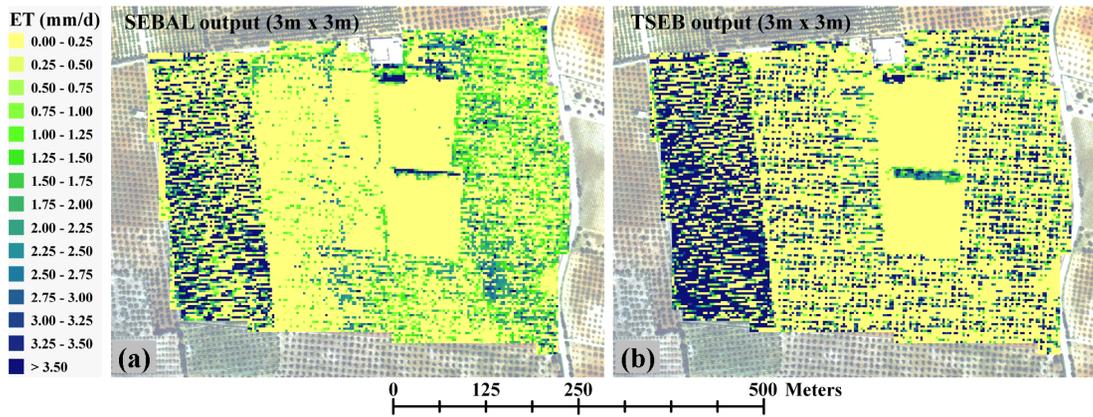
Fig. 6. Daily actual evapotranspiration map obtained from SEBAL model **(a)** and TSEB model **(b)**. (Both spatial distributions have a resolution of 3 m×3 m).

Estimation of Mediterranean crops evapotranspiration

M. Minacapilli et al.
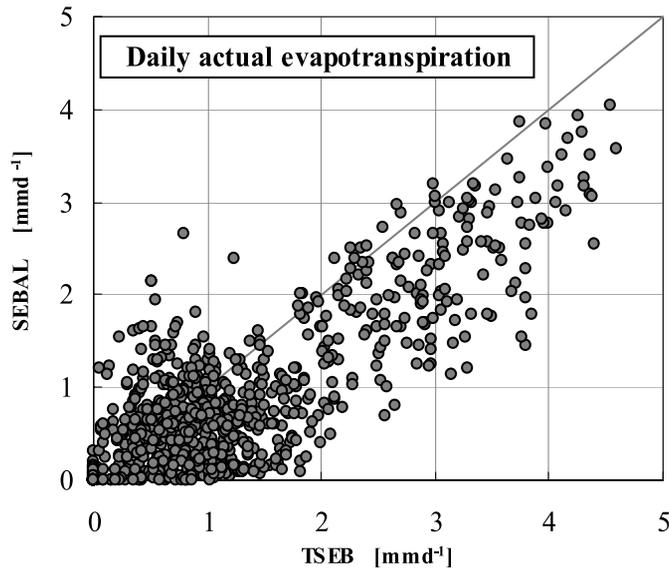
Fig. 7. Scatterplots of SEBAL versus TSEB evapotraspiration outputs.
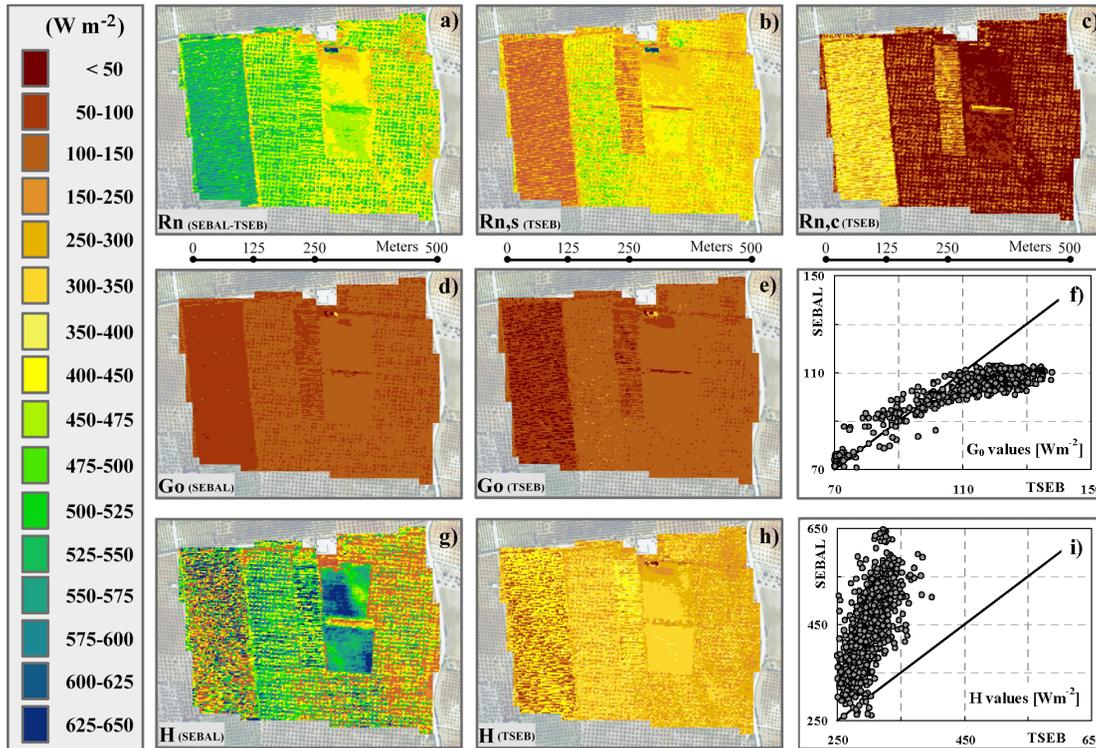
Fig. 8. Energy balance fluxes obtained using SEBAL and TSEB models; scatterplots of SEBAL versus TSEB soil heat flux, $G0$, **(f)** and sensible heat flux, H, **(i)**.
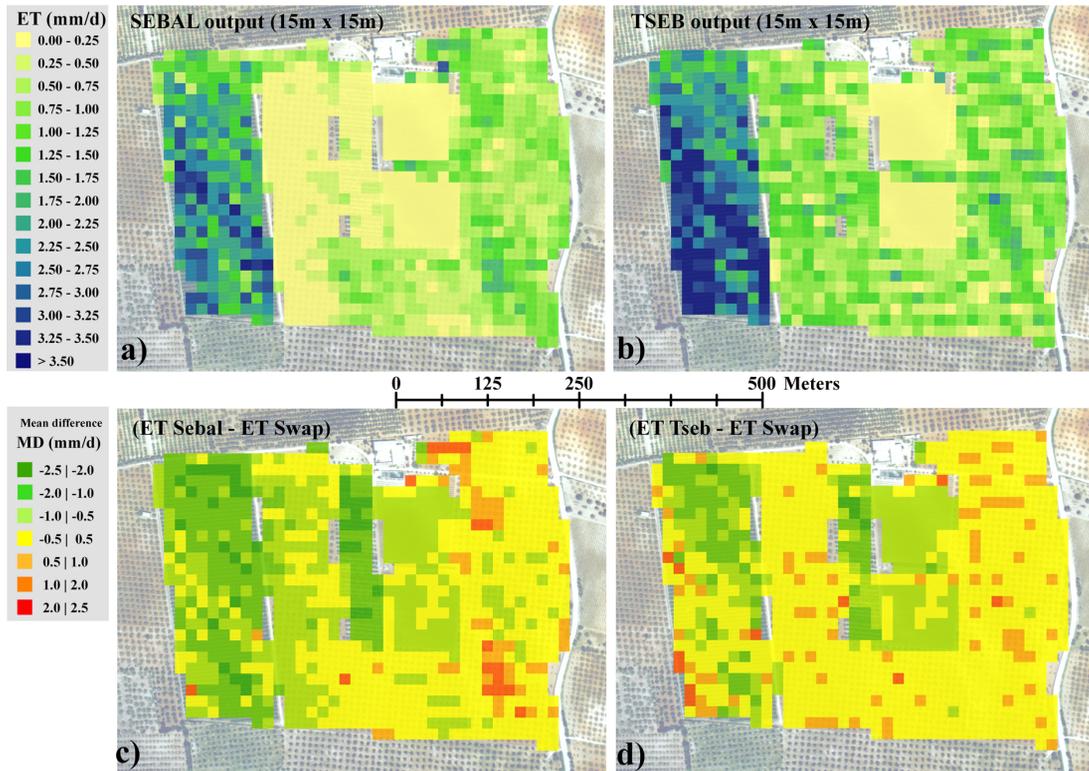
Fig. 9. Spatial distributions (15 m × 15 m resolution) of evapotranspiration rates obtained using **(a)** SEBAL and TSEB models. Differences values, MD, between **(c)** SEBAL and SWAP and **(d)** TSEB and SWAP modelled values.
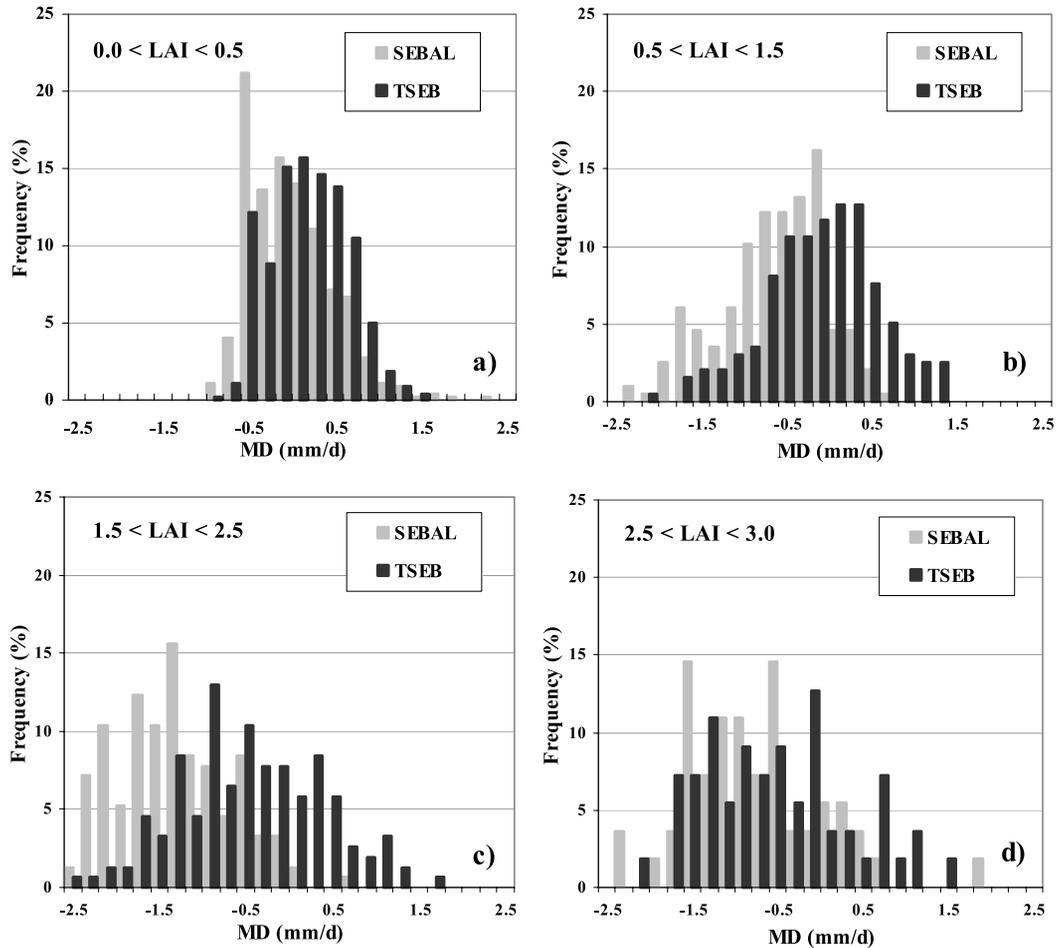
**Fig. 10.** Frequency distribution of difference values (MD) between SEBAL/TSEB and SWAP modelled evapotranspiration rates.
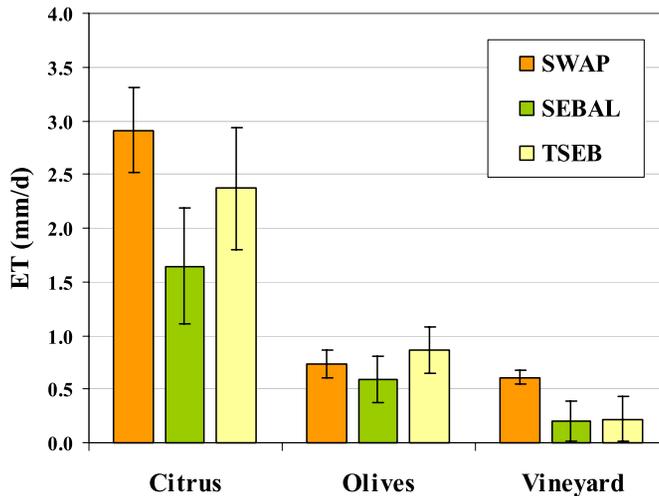
Fig. 11. Comparison between crop averaged evapotranspiration estimates (lines represent the range of +0.5 standard deviations).